The mobility of fluids through rocks

Bhavik Lodhia (b.lodhia@unsw.edu.au)
University of New South Wales Sydney
Stuart Clark

Article

Keywords:

Posted Date: December 10th, 2021

DOI: https://doi.org/10.21203/rs.3.rs-1126318/v1

Version of Record: A version of this preprint was published at Scientific Reports on June 17th, 2022. See the published version at https://doi.org/10.1038/s41598-022-14234-6.

The mobility of fluids through rocks

Bhavik Harish Lodhia[1] and Stuart Raymond Clark[1]

[1]Department of Minerals and Energy Resources Engineering, University of New South Wales, Sydney, 2052, Australia

November 30, 2021

Abstract

Over the last decade, there has been an irreversible shift from hydrocarbon exploration towards carbon storage, low-carbon energy generation and hydrogen exploration. Whilst basin modelling techniques may be used to predict the migration of hydrocarbons through sedimentary basins on geological timescales, there remains little understanding of how fluids behave at the basin scale on present-day timescales. Maximum vertical fluid velocity, v_{max}, may be calculated as the product of mobility and buoyancy. We present an algorithm to determine the basin-scale mobilities of CO_2 and methane with depth for sandstone and carbonate. CO_2 and methane mobility and buoyancy increase by an order of magnitude at gas phase transitions and are significantly greater in sandstone than in carbonate. Critical properties of CO_2 cause fluid mobility and buoyancy to be sensitive to changes in surface temperature. v_{max} for CO_2 and methane are on scales of m/year. Our results indicate an optimal depth for CO_2 storage of below 0.59 km and 1.24 km when surface temperature $> 20^{\circ}$C and 0°C, respectively. v_{max} for hydrogen is approximately $2 - 10$ times greater than other hydrocarbon fluids and this will have important consequences for the future use of basin modelling software for determining hydrogen migration for exploration and storage.

1 Introduction

The last decade has seen an irreversible shift in research focus away from hydrocarbon exploration and towards low-carbon energy production. This is reflected by the prioritisation of natural gas production over the use of high-CO_2 producing energy sources such as oil and coal, by many developed economies across the world (e.g. United States[1] and Australia[3]). Shifting priorities have led many of the world's largest energy producing companies to commit towards achieving carbon net-zero by 2050.[7;20] Hence, there is a growing interest across industry and the scientific community at applying well known techniques for hydrocarbon exploration to low-carbon technologies, such as carbon capture and storage (CCS) and green hydrogen exploration. Development of these techniques is dependent on understanding how CO_2, hydrogen and other fluids migrate through rocks. Traditionally, the history of fluid movement (e.g. hydrocarbons) through rocks across geologic time-scales has been calculated by basin modelling: a process by which sedimentary basins and their associated fluids are investigated to determine if the past conditions were appropriate to fill potential reservoirs with hydrocarbons and preserve the potential reservoirs.[10] The ability to simulate the passage of fluids through rocks is of significant importance to both hydrocarbon exploration and low-carbon activities, such as CCS. A large portion of processing time in basin modelling is used to solve Darcy flow equations in each grid cell of the model. Two- and three-dimensional basin models may take several days to compute on a home computer. This could be improved by assigning a fluid velocity that is dependent on properties of the carrier rock and depth. However, determining the velocities of fluids through different rock types remains a significant challenge. The overwhelming majority of research on fluid flow through rocks is focused on laboratory studies of specific examples or case studies or unsuccessful application of basin modelling software to simulate real-time fluid flow.[14] As we shall see, the determination of fluid velocities in different rock types as function of depth will be of immense value to both basin and future modelling studies for hydrocarbon exploration, CCS and potentially green hydrogen exploration and storage.

In this study, we apply various Equations of State and bulk properties of common rock types to different fluids encountered within the subsurface to calculate the variation of physical properties (e.g. volume and viscosity) with depth and surface temperature. Depositional parameter values for two generalised rock types, sandstone and carbonate, are applied in this study.[10] For carbonate, parameter values for micrite are used. Depositional porosity (ϕ_0) values are 0.41 and 0.51 and compaction wavelengths are 3.22 km and 1.92 km for sandstone and carbonate, respectively.[10]

We present an algorithm to calculate maximum vertical velocity, v_{max}, as a function of depth from the Darcy flow equation (Equation 1). The results of this study may have important implications for the application of

basin modelling techniques to understand migration of non-hydrocarbon fluids and for threshold depths, below which fluids have low mobilities.

2 Fluid properties in rocks

The Darcy flow equation[10] defines fluid velocity as

$$v_{max} = -\frac{kk_{rp}}{\nu}|\nabla \mathbf{u}| \tag{1}$$

whereby k = rock permeability, k_r = relative permeability, ν = fluid viscosity and $|\nabla \mathbf{u}|$ = driving force. The quantity kk_r = effective permeability and kk_{rp}/ν is defined as fluid mobility. As Equation 1 does not account for direction, calculated velocities represent a maximum value (v_{max}) oriented in the direction of the driving force, $|\nabla \mathbf{u}|$. In the case of fluid flow in geological media, $|\nabla \mathbf{u}|$ = buoyancy:

$$|\nabla \mathbf{u}| = (\rho_w - \rho_f)g \tag{2}$$

whereby ρ_w = density of water, ρ_f = density of fluid and g = gravity (9.80665 m/s^2).[10] The mobility of a fluid is a function of both fluid properties and rock type of the carrier, whereas buoyancy is independent of rock type.

The terms of Equation 1 include several important quantities that must be evaluated separately using the appropriate relationships that describe fluid volume, viscosity, density and buoyancy.

Fluid properties and buoyancy

The primary driving force responsible for fluid flow in the geological media is buoyancy, which depends on several factors including fluid and rock properties. Fluid properties are described by Equations of State (EoS), which define the relationship between pressure, volume and temperature. The most well known EoS is the Ideal Gas Equation, however such a simple relationship does not accurately model properties of non-ideal fluids (e.g. CO_2 and methane) and cannot be used in complex scenarios such as geological basin modelling. There are numerous widely used EoS that describe the realtionship between fluid pressure, temperature and volume for non-ideal molecules. The Peng-Robinson 1978 (PR78)[18] and Soave-Redlich-Kwong (SRK)[21] EoS are known for their accuracy for multi-phase and multi-component fluids at pressures < 100 MPa and temperatures between 300°K -500°K, covering the conditions exhibited in most geological basins across the world. Other EoS that may be used include the Reidlich-Kwong (RK) EoS, which is suited for small, non-polar and short-chained molecules.[5;6;26;16] Other EoS have been developed specifically for use with hydrocarbons[24;25], e.g. volatile, light and black oils. Component properties for CO_2, methane, hydrogen, dry gas, wet gas and hydrocarbon fluids are listed on Table 1.

	M_W [g/mol]	T_c [^{o}K]	P_c [MPa]	v_c [m^3/kmol]	ω
CO_2	44.010	304.19	7.382	0.0940	0.2276
Methane	16.043	190.56	4.599	0.0985	0.0115
Dry gas	17.943	197.42	4.850	0.0977	0.0221
Wet gas	30.186	272.40	4.801	0.1345	0.0624
H_2	2.016	33.18	1.313	0.0642	-0.215
Volatile oil	53.135	367.79	4.372	0.1956	0.1267
Light oil	48.439	357.38	4.389	0.1895	0.1238
Black oil	90.072	491.62	3.535	0.2423	0.3121

Table 1: Component properties of hydrocarbon gases, hydrogen and CO_2.[9;10;13;17] $M_{W=}$ molecular weight, T_C = critical temperature, P_c = critical temperature, v_c = critical volume, ω = acentric factor.

Whilst EoS may be applied to calculate fluid pressure, temperature and volume, viscosity is another important indicator for phase property characterisations and fluid velocities within rocks and geological basins. Viscosity is often modelled as a quantity dependent only on pressure, temperature, density and the amount of dissolved gas.[9] Whilst advanced theories, such as the friction-theory or free-volume model match laboratory data well, a lack of field data and unknown component parameters (especially for heavy hydrocarbon compounds) make these unsuitable for basin modelling.[10]

Compared to methods that require laboratory or field data, direct approaches such as the empirical Lohrenz–Bray–Clark (LBC) model[15;5;6] are simpler to apply in basin modelling scenarios where data is often scarce. Viscosities can be evaluated very fast due to the simple nature of the LBC–formulas. However, models with lower performance are often not usable in fluid flow simulators. It must also be noted that the LBC-model is based on a polynomial

of degree 16. Polynomials of such a high degree are known to easily become numerically unstable and therefore LBC-based models must be evaluated with care.[10] Furthermore, the pressure correction for gases in the LBC method had a tabular formula and was not presented entirely.[15] Using this distinction introduces a discontinuity between the liquid and gas viscosity. A modification to the LBC method may be made by applying the Herning mixing rule.[11] This was validated to successfully model multicomponent and multiphase fluid viscosity using the modified LBC approach for an example using the independent Stiel-Thodos method.[6;22] Hence, this modified LBC method is preferred over the original LBC method.[6;15]

The range of pressure and temperature (PT) paths in in Figure 1 defines an area of possible PT points in arbitrary sedimentary basins. To simulate generic geological conditions, a geothermal gradient of 25°C/km and PT gradient for normal conditions (0.5 MPa/K) was applied (Figure 1[10]) to calculate the molar volume and density of CO_2 and methane by solving the PR78, SRK and RK EoS.[5;6] The modified-LBC method[6] was used to calculate fluid viscosity (Figure 2).

The transition between phases (solid, dense liquid, liquid, gas and supercritical fluid) is controlled by a fluid's pressure and temperature relative to its critical pressure (P_c) and temperature (T_c). Figure 3 shows phase diagrams of CO_2 and methane with PT paths for $T_s = 0$°C and 20°C. For CO_2, $P_c = 7.3773$ MPa and $T_c = 30.98$°C and is encountered at 0.59 km under normal geological conditions. When $T_s < 20$°C, CO_2 undergoes three phase transitions at 0.36 km (gas-liquid), 0.59 km (liquid-dense liquid) and 1.24 km (dense liquid-supercritical). However, when $T_s \geq 20°$ C, only one phase transition occurs at 0.59 km (gas-supercritical). For methane, all conditions within the Earth irrespective of T_s place PT paths within the gas-supercritical region and only one phase transition occurs at 0.36 km.

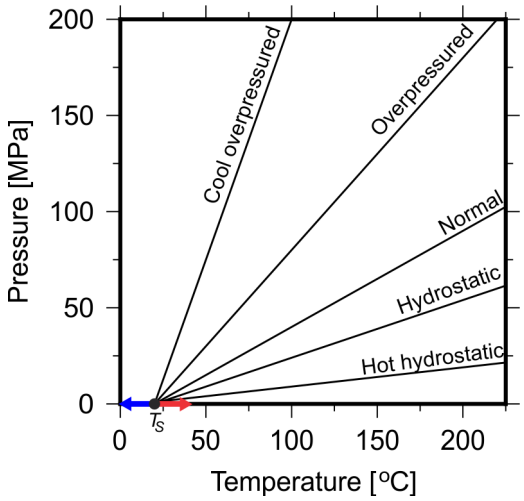

Figure 1: Typical pressure temperature (PT) paths in geological basins with a surface temperature of 20°C.[10] PT gradients are as follows: cool and overpressured = 2.5 MPa/K, overpressured = 1.0 MPa/K, normal = 0.5 MPa/K, hydrostatic = 0.3 MPa/K and hot hydrostatic = 0.1 MPa/K.

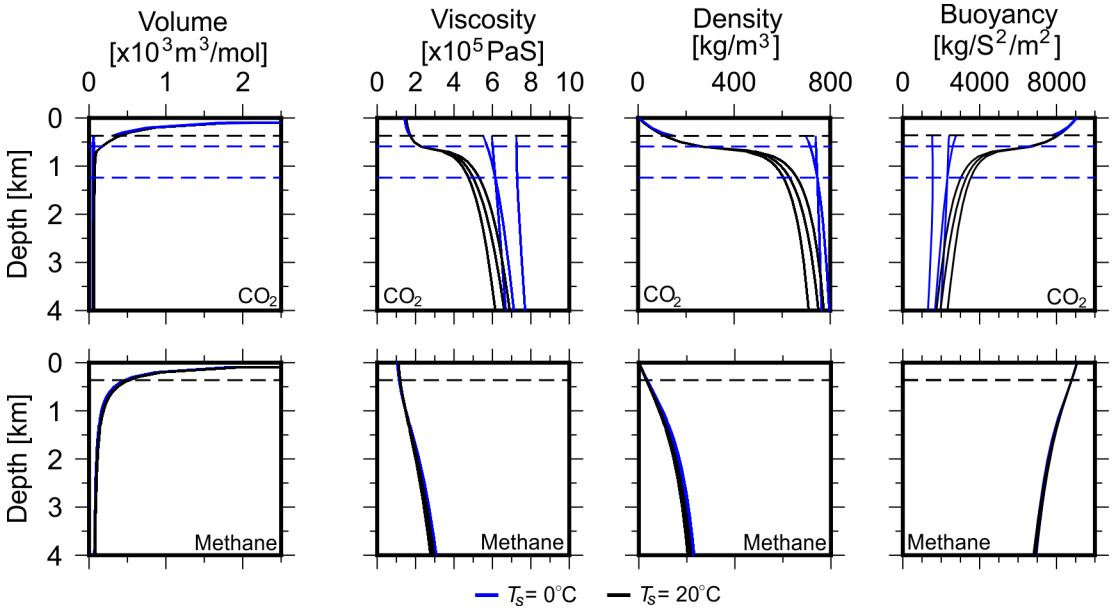

Figure 2: Fluid molar volume, viscosity, density and buoyancy calculated using various Equations of State and modified-LBC method[6;5] and surface temperature of 20°C. Blue and black lines represent values calculated using PR78[18], SRK[21] and Reidlich-Kwong[26;16] EoS at $T_s = 0$°C and 20°C, respectively. Blue dashed lines represent supercritical-dense liquid and dense liquid-liquid phase transitions for $T_s = 0$°C. Black dashed lines represent gas-supercritical phase transition for $T_s = 20$°C (see Figure 3). The change from liquid to gas for all fluids is marked by an exponential increase in molar volume and decreases in viscosity and density.

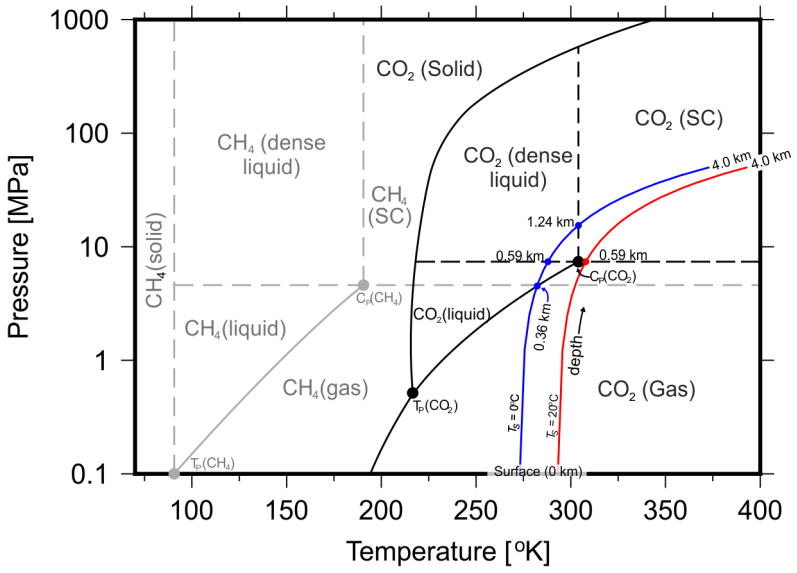

Figure 3: Phase diagram for CO_2, methane calculated at normal geological conditions and geothermal gradient = 25°C/km. Blue and red lines represent PT paths calculated at T_s = 0°C and 20°C, respectively. Black lines and points represent phase diagram for CO_2. grey lines and points represent the phase diagram for methane. T_p = triple point, C_p = critical point.

Porosity, permeability and saturation

The velocity of fluids in rocks (e.g. sandstone and carbonate) depend on a number of factors, including properties of fluids (Table 1) and rocks (Figure 4). Another important parameter is porosity, ϕ, and is defined as the ratio of free pore space to rock volume. ϕ controls the volume between grains in a sedimentary rock which may hold fluids and reduces as with compaction. The variation of ϕ with depth must be considered when evaluating fluid velocities through rocks. Athy's relation[2] parametrises ϕ using:

$$\phi = \phi_0 e^{-z/k} \tag{3}$$

whereby ϕ_0 is the maximum (depositional) porosity and k is the Athy compaction parameter (Table 2).

The flow of fluids through rocks generally involves more than a single phase. The ability of one fluid to flow through a rock or reservoir is affected by the presence of other fluids. Relative permeability, k_{rp} describes multiphase flow in reservoirs as the ratio of the effective permeability of a fluid to the absolute permeability of the rock. The effective permeability is a relative measure of conductance of the porous medium for one fluid phase in the presence of other fluid phases.

Vertical and horizontal rock permeabilities may be calculated from hand-specimen measurements by using appropriate anisotropy and upscaling factors. Anisotropy is the ratio of horizontal and vertical permeability and is dependent on rock type. Basin scale values for horizontal and vertical permeabilities are calculated from hand specimen values multiplied a horizontal and vertical upscaling factor, respectively. The resulting higher values for larger scales are caused by macro-fractures, inhomogeneities and permeable inclusions.[10] Here, we apply typical upscaling factors of 1 (vertical) and 50 (horizontal). However, greater upscaling factors (e.g. vertical = 10 and horizontal = 500) to basin scale elements with lengths greater > 50 m are reported in the literature for sandstones.[19]

Name	a_k	Porosity at point			Permeability [logmD] at point			Athy k [km]	Athy k [MPa]
		1	2	ϕ_0	1	2	ϕ_0		
Sandstone	5	0.01	0.25	0.41	-1.8	3	4.33	3.225	37.593
Carbonate	1.1	0.01	0.25	0.51	-2.20	1.00	1.52	1.923	20.982

Table 2: Rock properties. Anisotropy = a_k. Porosity and permeability values used to generate multipoint curves and rock saturation endpoint values for bulk rock. ϕ_0 = maximum (depositional) porosity of rock.[10] These values were used to determine the rock permeability from porosity shown on Figure 4.

Numerous models for estimating relative permeability have been proposed over the last half century. Most relative permeability models[4] assume relative permeability to be a function of connate water saturation (S_w)

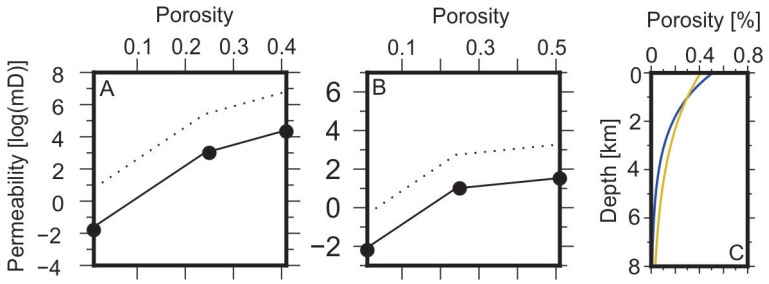

Figure 4: Upscaled rock permeability and porosity. Values from Table 2 are used to calculate rock permeability between maximum (depositional) porosity and zero.[10] A = sandstone, B = carbonate. Solid and dotted lines represent vertical and horizontal permeability, respectively. C = porosity-depth relationship calculated using Athy's relation.[2] Gold and blue lines represent sandstone and carbonate, respectively.

and connate gas saturation (S_g) respectively. The relative permeability of any fluid is zero below its critical saturation, where it becomes immobile. Saturations are for often rescaled into normalised or effective saturations (S_e) which map the saturation interval between the connate and the critical saturation to an interval of $0 < S_e < 1$. The relationships between normalised saturations of water, S_{we}, gas, S_{ge} and oil-gas, S_{goe}, are as follows:

$$\begin{array}{lll} S_{we} = (S_w - S_{wc})/(1 - S_{wc} - S_{oc}) & \text{for} & k_{rw}, k_{row} \\ S_{goe} = S_g/(1 - S_{wc}) & \text{for} & k_{rog} \\ S_{ge} = (S_g - S_{gc})/(1 - S_{wc} - S_{gc}) & \text{for} & k_{rg} \end{array} \quad (4)$$

whereby k_{rw}, k_{row}, k_{rog} and k_{rg} are the relative permeabilities of water, oil-water, oil-gas and gas components respectively. k_{rw} and k_{rog} represent water-liquid flow whilst k_{rg} and k_{rog} represent liquid-vapour flow, respectively. Hence, $k_{rw} = f(S_w)$, $k_{rg} = f(S_g)$, $k_{row} = f(S_w)$ and $k_{rog} = f(S_g)$. Assuming that phases do not interact during flow[4], the flow of each phase can be treated as if the other phases are part of the solid rock matrix. In this case, the relative permeability of oil, $k_{ro} = k_{row}k_{rog}$. We use this relationship to approximate the flow of the fluids (Table 1) in sandstones and carbonates.

Water saturation from porosity

Determining water saturation, S_w, is an extremely challenging petrophysical calculation to perform. S_w is used to quantify the hydrocarbon saturation, $(1 - S_w)$ and must be evaluated in basin modelling. Complexities arise because there are a number of independent approaches that can be used to calculate S_w. In wellbores, the following methods can be used to determine S_w:

- S_w calulations from resistivity logs and by application of a model relating S_w to porosity, ϕ, connate water resistivity and lithology-dependent electrical properties.
- S_w calculations from laboratory capillary pressure and saturation (P_{cap}/S_w) measurements by application of a model relating S_w to various rock, fluid properties and height above the free-water level.
- S_w calculations using oil-based mud (OBM)-core-plug Dean-Stark-water-volume determinations.
- Combinations of these methods

The amount of data that is available often dictates which method to use to determine S_w. For the purposes of basin modelling, which requires the application of generalised lithologies and fluid types, S_w must be calculated from data input by the user, e.g. rock type, fluid type and depth. Laboratory-based methods for measuring S_w are not suitable for this work, as we are concerned with the properties of generalised rock types and fluids on the basin-scale.

The results of early experiments[8] indicated that the product of ϕ and S_w is constant. The magnitude of this constant was shown to be a related to rock type and indirectly to permeability, k. Better quality rocks were found to correspond with low constant values. Extensive analysis of core data and petrophysical estimates of porosity and irreducible water saturation[12], from all types of reservoirs worldwide, suggests that this relation[8] is a unique solution to a more general equation:

$$\phi^Q \times S_w = C \quad (5)$$

whereby the value of the power function Q ranges from 0.8 to 1.3, with many reservoirs close to 1.0. For sandstones, $0.02 < C < 0.10$ and $0.005 < C < 0.06$ for carbonates. The values of Q and constant C can be

easily derived by plotting logϕ against logS_w. The gradient of this linear plot = Q. Projection of the straight line against $\phi = 1.0$ gives the value of the constant, C.[12] Figure 5 shows the relationship between S_w and ϕ calculated using Equation 5 and depth from Equation 3. Uncertainties may be calculated using the upper and lower bounds of experimental constants and exponent terms from laboratory measurement.[12] Uncertainty increases significantly as porosity is reduced through compaction ($\phi < 5\%$) and with depth. Uncertainties increase significantly below 3 km and cover almost the entire range of possible S_w values by 4 km depth. Hence, we have limited our modelling to this depth.

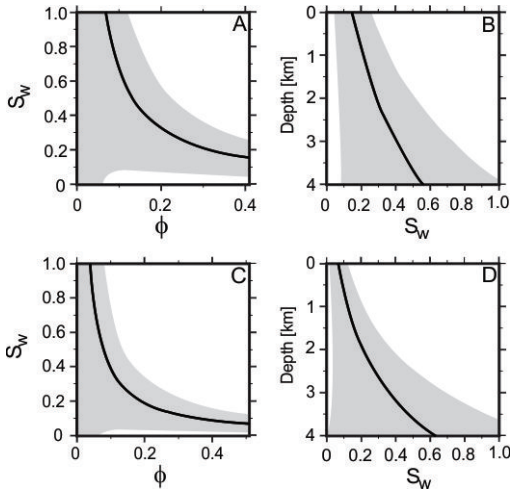

Figure 5: Connate water saturation (S_w) as a function of porosity and depth calculated using parameters for sandstone and carbonate[10;12] and Athy's relation.[2] A-B = sandstone, C-D = carbonate. Grey regions represent uncertainties calculated using upper and lower bounds of experimental constants for Equation 5[12]. Uncertainties beyond depths of 4 km represent the full range of possible S_w values hence we do not extend this method beyond this depth.

3 Fluid mobility in rocks

Using Athy's relation[2] and the values in Tables 1 and 2, we use the following algorithm to calculate the vertical mobility and buoyancy of CO_2 and methane:

(1) Solve chemical equation of state (EoS) to calculate fluid volume from pressure and tempearature
(2) Calculate rock porosity (ϕ) and permeability at depth
(3) Calculate fluid-water relative permeability (k_{rp}) and connate water saturation (S_w) from porosity (6)
(4) Calculate fluid viscosity from pressure and temperature
(5) Calculate vertical fluid mobility and buoyancy

The results for fluid mobility and buoyancy calculations for CO_2 and methane at normal geological conditions for surface temperatures of 0°C and 20°C are shown on Figure 6. Gas phase mobility increases exponentially as depth decreases, with maximum mobility at the surface. Non-gas phase mobilities for both CO_2 and methane in both sandstones and carbonates are significantly lower than corresponding gas phase mobilities and decrease exponentially with depth. Fluid buoyancy follows a similar pattern.

The choice of EoS has a minimal impact on calculated fluid mobility and buoyancy for CO_2 and methane. Fluid buoyancies increase exponentially upon the transition to gas phase. Methane mobility varies little with T_s, with results indistinguishable for T_s = 0°C and 20°C. Calculated vertical fluid mobilities for CO_2 are particularly sensitive to T_s. Fluid mobilities for both CO_2 and methane are approximately double in sandstone compared to carbonate. Whilst the magnitude of vertical mobilities of fluids vary little with surface temperature, the depth of liquid-gas phase transitions vary considerably where critical properties are close to surface conditions (Figure 3).

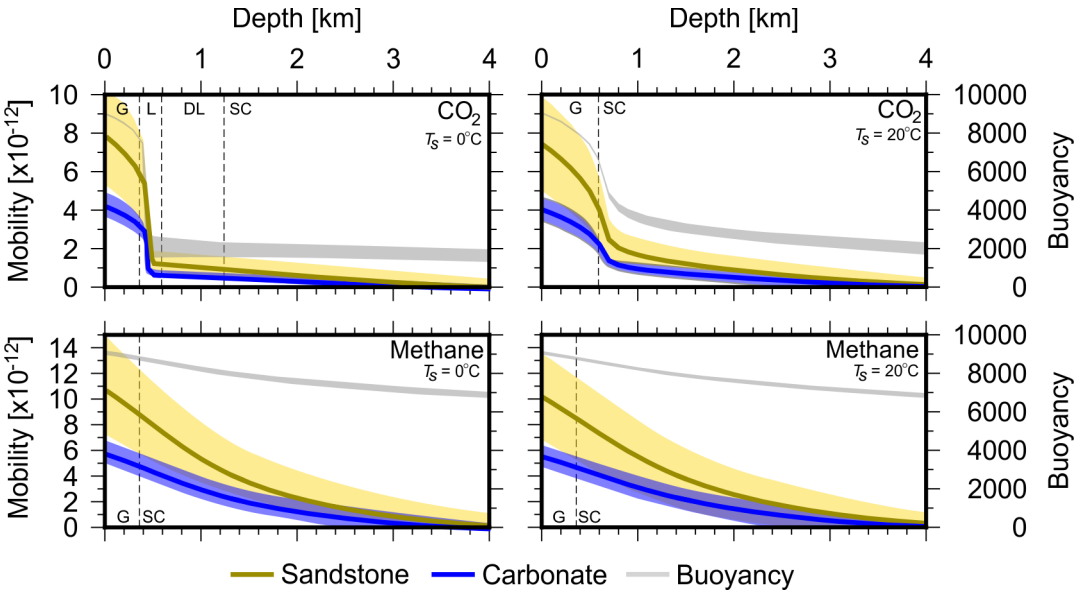

Figure 6: Fluid mobility for CO_2 and methane calculated according to Equation 1. Units for fluid mobility are m^2 Pa^{-1} S and buoyancy are m^3 S kg^{-1}. Yellow and blue lines represent fluid mobility in sandstone and carbonate, respectively. Grey lines represent buoyancy and shaded regions represent range of values calculated using different EoS and lithological parameters for Equation 5. Dashed lines represent phase transitions: G = gas, L = liquid, DL = dense liquid and SC = super-critical.

The equations used to relate relative permeability and normalised water saturation (Equation 4) are designed for application to fluid systems with water, oil-water and gas-oil components. However, it is intriguing to extend this analysis to other fluids. The properties of several other important hydrocarbon fluids and hydrogen are listed in Table 1. We apply the algorithm proposed in this study to calculate vertical fluid mobility and buoyancy for hydrogen, dry/wet gas and various hydrocarbon fluids (Figures 8 and 7).

Unlike for CO_2, the vertical fluid mobilities and buoyancies of all other fluids considered in this study do not show significant sensitivity to T_s. The magnitude of vertical fluid mobilities of hydrogen are up to twice those of dry/wet gas and over an order of magnitude greater than other hydrocarbon fluids (volatile, light and black oil). The buoyancy of hydrogen varies little with depth as all conditions within the Earth are beyond its critical parameters. Whilst above 0.36 km, the buoyancy of hydrogen is close to that of other gas phase fluids (methane, dry and wet gas, Figure 8) and is > 8000 $m^3S^{-1}kg^{-1}$. Hence, this raises the important consideration that hydrogen velocities may be $2 - 10$ times greater than those for other fluids and must be accounted for when evaluating hydrogen migration whilst applying conventional fluid flow modelling techniques suited for hydrocarbon migration. The vertical fluid mobilities for volatile, light and black oils are an order of magnitude smaller than those for other fluids, reflecting the fact that these remain in the liquid phase at all levels below the surface. Whilst results for dry gas are close to those for methane, results for wet gas resemble the pattern seen for CO_2 when $T_s = 20°C$. This is expected, as conditions within the Earth exceed the critical properties of wet gas (Table1).

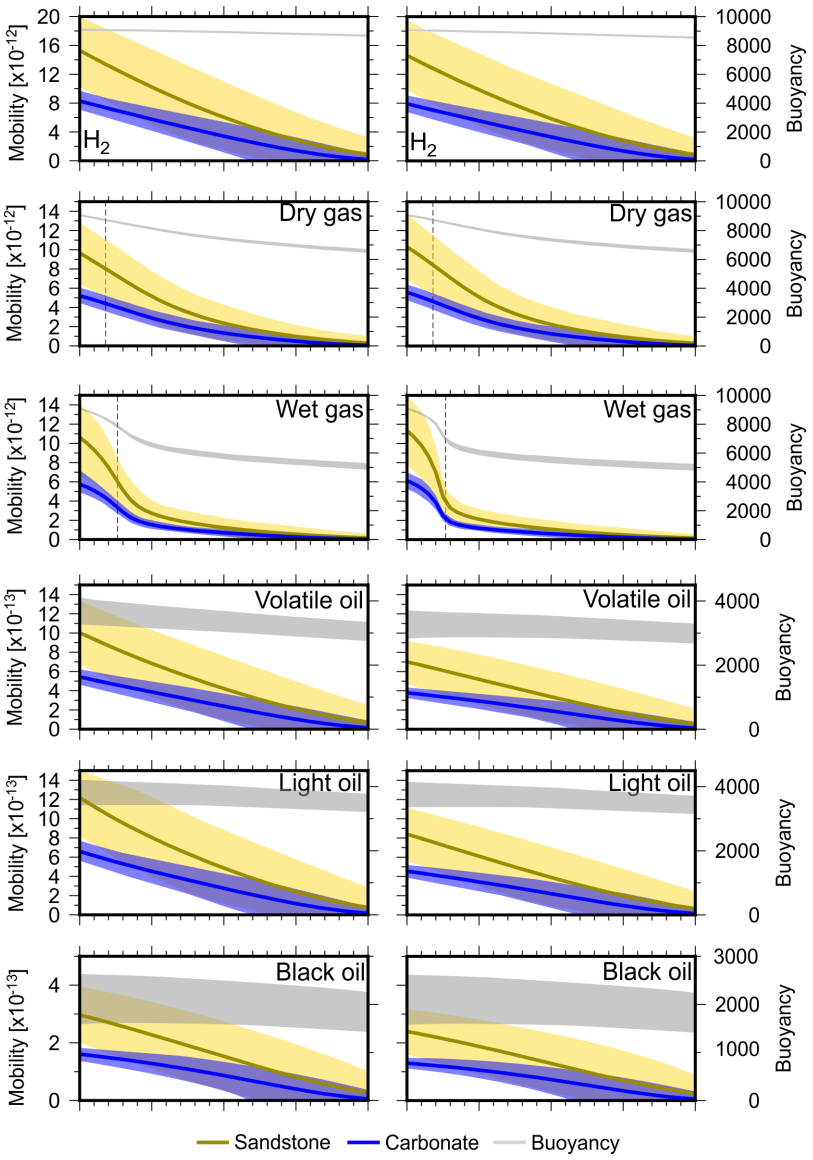

Figure 7: Fluid mobility for non-hydrocarbon and hydrocarbon fluids listed in Table 1 calculated according to Equation 1. Units for fluid mobility are m^2 Pa^{-1} S and buoyancy are m^3 S kg^{-1}. Yellow and blue lines represent fluid mobility in sandstone and carbonate, respectively. Grey lines represent buoyancy and shaded regions represent error. Wet and dry gas exhibit similar properties to CO_2 and methane, respectively. Phase transitions for CO_2 and methane are plotted on wet and dry gas, respectively as dashed lines.

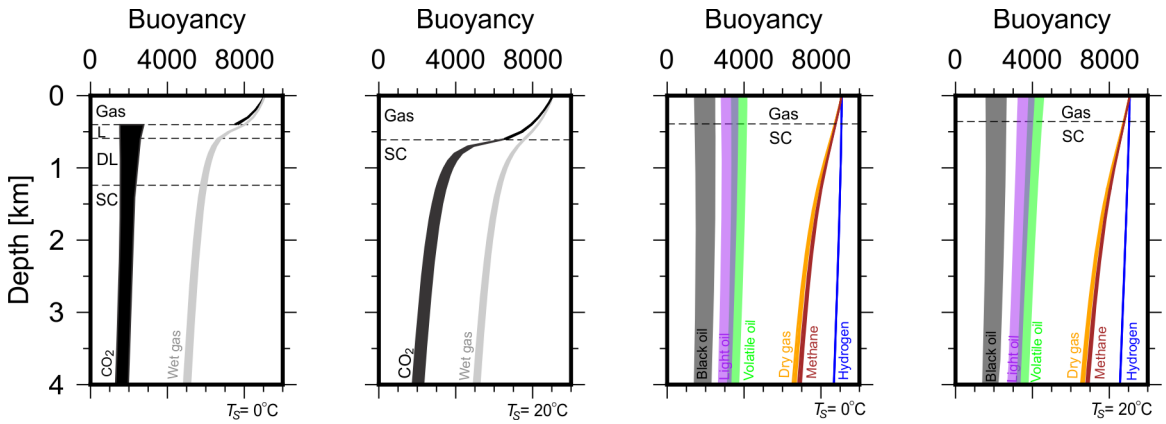

Figure 8: Fluid buoyancy calculated for other hydrocarbon and non-hydrocarbon fluids listed on Table 1 calculated using PR78[18], SRK[21] and RK[5;6;16;26?] EoS for dry/wet gas and hydrogen and using appropriate EoS for hydrocarbon fluids.[24;25] Wet gas exhibits similar properties to CO_2 at $T_s = 20°C$, whilst dry gas exhibits similar properties to methane. Hydrocarbon fluid buoyancies are significantly lower than dry gas and methane and decrease with molecular weight. Hydrogen buoyancy varies little with depth.

4 Discussion

The results of this study have several important implications. The velocity of fluids through rocks may be calculated directly by multiplying vertical fluid mobility and buoyancy, according to Equation 1. Results indicate maximum vertical gas-phase velocities of $1.5 - 4$ m/year (sandstone) and $1 - 2.5$ m/year (carbonate) for CO_2 and methane, respectively. As both vertical fluid mobility and buoyancy decrease exponentially below the gas-supercritical or gas-liquid phase transition, our results indicate a minimum depth for CO_2 storage 0.36 km and 0.59 km when $T_s = 0°C$ and 20°C, respectively.

The methodology presented in this study if combined with a directional vector, may provide a fast and computationally inexpensive means to calculate fluid velocities as a function of depth and angle of incidence between fluid particles and geological horizons, e.g. impermeable seals. A potential method to calculate the direction of fluid flow beneath geological seals is flowpath bending, which is widely used to model petroleum flow in basin modelling software. A planar seal with dipping angle α in the y–direction and lateral water flow with angle β to the x–axis and a hydraulic head with a dipping angle of γ are used to define the angle ψ, which indicates the direction of fluid flow as[10]:

$$tan\phi = tan\beta cos^2\alpha \frac{\Delta\rho}{\rho_w} \frac{cos\alpha sin\alpha}{tan\gamma cos\beta} \tag{7}$$

whereby $\Delta\rho$ = difference in density between fluid and water and ρ_w = water density. When water flow is also assumed to follow the dipping of the seal, this becomes[10]:

$$tan\phi = tan\beta \frac{\Delta\rho}{\rho_w} \sqrt{1 + sin^2\beta tan^2\alpha} \frac{cos\alpha sin\alpha}{tan\gamma cos\beta} \tag{8}$$

Combining calculations for v_{max} and directional vectors could significantly reduce fluid flow simulation processing time compared to leading basin modelling software packages that rely on the creation of nodal meshes to process fluid particle-rock interactions.

Modelling of CO_2 and H_2 storage are dependent on understanding the present-day velocities of fluids, however there exists no direct method for calculating fluid velocities as a function of lithology and depth. Attempts to apply basin modelling software to predict the effect of fluid injection on basin-scale pressure evolution have been largely unsuccessful.[14] Whilst the assumptions used in this work are relevant for water, oil or gas fluid systems in generalised sandstones and carbonates, our results could have important implications for future investigations for carbon storage and hydrogen exploration.

Sedimentary basins around the world are often characterised by complex geological histories. The PT-path of sedimentary basins will likely cross several regimes (e.g. different lines on Figure 1). The methodology outlined in this study may be used to evaluate fluid velocities through different geological regimes (e.g. moving from normal conditions to regions of overpressure) by choosing the appropriate PT-path for discrete depth intervals. Future work should focus on expanding our understanding about the relationship between porosity and water saturation[12] in different rock types. New experimental data for a wide range of rock types will improve Equation 5 and broaden the possibilities for the methodology described in this study.

It is widely accepted that hydrocarbons have the capability to migrate long distance through carriers on geological timescales, which indicative vertical fluid velocity calculations in literature reported at 180 km/Ma (0.18 m/year).[10] The results of this work indicate that CO_2, methane, dry gas, wet gas and H_2 may migrate several metres vertically per year (> 1000 km/Ma) when in the gas phase. It is very encouraging that these values are consistent in magnitude with reports in the literature of hydrocarbon velocities of up to 1000 km/Ma[23], and indicate that the approximations used in this method are appropriate. Our results also indicate that future application of basin modelling techniques and software to explore for hydrogen should account for hydrogen fluid velocities that are approximately $2 - 10$ times that of hydrocarbons at the same geological conditions. It is encouraging that exponential increases in fluid velocities are concomitant with liquid-gas phase transitions given that this is independent of rock type. Furthermore, the magnitudes of vertical match those reported for hydrocarbon fluids that are of similar composition and molecular weights to the fluids analysed in this study (excluding H_2).

5 Conclusions

We present an algorithm to calculate vertical fluid mobility and buoyancy for CO_2 and methane as a function of depth for generic sandstone and carbonate by combining solutions to chemical equations of state, viscosity and permeability calculations and the Darcy-Flow equation. Vertical fluid mobility and buoyancy in both sandstone

and carbonate decrease exponentially with depth and are significantly greater for gas phases compared to liquid, dense liquid or supercritical phases. The depth of the phase transitions for CO_2 is sensitive to surface temperature, whereby gas-liquid and gas-supercritical transitions occur at 0.36 km for $T_s = 0°C$ and 0.59 km for $T_s = 20°C$, respectively. Surface temperatures $> 0°C$ push the pressure-temperature profile of CO_2 into the gas-supercritical region. Hydrogen velocities may be approximately $2 - 10$ times greater than those of CO_2, methane, dry and wet gas and over an order of magnitude greater than for other hydrocarbon fluids. Dry and wet gas follow similar trajectories as methane and CO_2. Vertical fluid mobility and buoyancy of other hydrocarbon fluids (volatile, light and black oil) are an order of magnitude smaller than those of CO_2, methane and dry/wet gas.

6 Acknowledgements

This work was supported by the Australian Research Council grant number GA85582. Special thanks are given to Dr Juerg Hauser (CSIRO) and Mr Zakhar Lanetc (UNSW) for their discussions during the completion of this work.

References

[1] U.S. Energy Information Administration. Natural gas explained, Where our natural gas comes from, 2021.

[2] L. F. Athy. Density, Porosity, and Compaction of Sedimentary Rocks. *AAPG Bulletin*, 14(1):194–200, 1930.

[3] Geoscience Australia. Australia's Energy Commodity Resources, 2021. 2021.

[4] K. Aziz and A. Settari. Petroleum Reservoir Simulation, 1979.

[5] C. Bell. chemicals: Chemical properties component of Chemical Engineering Design Library (ChEDL), 2021.

[6] C. Bell. Thermo: Chemical properties component of Chemical Engineering Design Library (ChEDL), 2021.

[7] British Petroleum. BP sets ambition for net zero by 2050, fundamentally changing organisation to deliver. *BP press*, 2020.

[8] R.S. Buckles. Correlating and Averaging Connate Water Saturation Data. *Journal of Canadian Petroleum Technology*, 4(01):42–52, 1965.

[9] A. Danesh. PVT and phase behaviour of petroleum reservoir fluids. In *Number 47 in Developments in petroleum science*. Elsevier, 1998.

[10] T. Hantschel and A.I. Kauerauf. *Fundamentals of Basin and Petroleum Systems Modeling*. Springer, 2009.

[11] F. Herning. *Beitrag zur Berechnung der Zähigkeit technischer Gasgemische aus den Zähigkeitswerten der Einzelbestandteile*. Dipl. ing, Oldenbourg, 1935.

[12] Michael Holmes, Antony Holmes, and Dominic Holmes. Relationship between Porosity and Water Saturation : Methodology to Distinguish Mobile from Capillary Bound Water Two different rock types. *AAPG Annual Convention*, 110108:1–11, 2009.

[13] IES PetroMod®. Petroleum Systems Modeling Software, Release 10.0, 2007.

[14] C. Ihrig and V. Unnithan. Feasibility Study of Using a Petroleum Systems Modelling Software to Evaluate Basin Scale Pressure Evolution Associated with CO2 Storage. In G. Lohmann, K. Grosfeld, D. Wolf-Gladrow, A. Wegner, J. Notholt, and V. Unnithan, editors, *Geoengineering. In Earth System Science: Bridging the Gaps between Disciplines*. Springer, Berlin, Heidelberg, 2013.

[15] John Lohrenz, Bruce G. Bray, and Charles R. Clark. Calculating Viscosities of Reservoir Fluids From Their Compositions. *Journal of Petroleum Technology*, 16(10):1171–1176, 1964.

[16] B.E. Poling. *The Properties of Gases and Liquids*. McGraw-Hill Professional, New York, 5 edition, 2000.

[17] R. C. Reid, J.M. Prausnitz, and B.E. Poling. *The Properties of Gases and Liquids*. McGraw–Hill Book Company, 4 edition, 1987.

[18] Donald B Robinson and Ding-Yu Peng. The Characterization of the Heptanes and Heavier Fractions for the GPA Peng-Robinson Programs. In *Gas Processors Association*, Tulsa, Oklahoma, 1978.

[19] D. Schulze-Makuch, D.A. Carlson, D.S. Cherkauer, and P. Malik. Scale Dependency of Hydraulic Conductivity in Heterogeneous Media. *Ground Water*, 36(6):904–919, 1999.

[20] Royal Dutch Shell. Shell accelerates drive for net-zero emissions with customer-first strategy, 2021.

[21] Giorgio Soave. Equilibrium constants from a modified Redlich-Kwong equation of state. *Chemical Engineering Science*, 27(6):1197–1203, 1972.

[22] Leonard I. Stiel and George Thodos. The viscosity of nonpolar gases at normal pressures. *AIChE Journal*, 7(4):611–615, 1961.

[23] Ø. Sylta. *Hydrocarbon Migration Modelling and Exploration Risk*. Phd, Norwegian University of Science and Technology, 2004.

[24] Chorng H. Twu, John E. Coon, and John R. Cunningham. A new generalized alpha function for a cubic equation of state Part 1. Peng-Robinson equation. *Fluid Phase Equilibria*, 105(1):49–59, 1995.

[25] Chorng H. Twu, John E. Coon, and John R. Cunningham. A new generalized alpha function for a cubic equation of state Part 2. Redlich-Kwong equation. *Fluid Phase Equilibria*, 105(1):61–69, 1995.

[26] S.M. Walas. *Phase Equilibria in Chemical Engineering*. Butterworth-Heinemann, 1985.